Received: Added at production | Revised: Added at production | Accepted: Added at production

DOI: xxx/xxxx

MANUSCRIPT

Capillary Density and Neuronal Homeostasis in Human Primary Visual Cortex

Yi-Chung Wang[1] | Amy Guo[1] | Adam JH Newton[1,2] | Robert A McDougal[1] | William W Lytton[2,3] | Marcello M DiStasio[4,5]

[1]Department of Biostatistics, Yale School of Public Health, New Haven, CT, United States

[2]Department of Physiology and Pharmacology, SUNY Downstate Health Sciences University, Brooklyn, NY, United States

[3]Department of Neurology, Kings County Hospital Center, Brooklyn, NY, United States

[4]Department of Pathology, Yale School of Medicine, CT, United States

[5]Department of Ophthalmology and Visual Science, Yale School of Medicine, CT, United States

Correspondence
Marcello DiStasio
300 George St. Rm. 353D
New Haven, CT 06511.
Email: marcello.distasio@yale.edu

Abstract

Hypoxia is a pathological condition associated with spreading depolarization. Although neuronal density has been widely explored across brain regions, the distribution of distances between neurons and vasculature plays an important role in the availability of free oxygen to neurons to support their metabolism, which in turn supports maintenance of resting membrane potential.

This study analyzes the distribution of distances between neurons and vasculature in the primary visual cortex of humans, using post-mortem samples of normal primary cortex from 3 subjects ages 65-75. We performed dual-label immunohistochemistry with antibody markers for NeuN (for neurons) and CD34 (for vascular endothelial cells). Region of interest (ROIs) of neocortical layers were delineated manually by a neuropathologist. Within these regions, object-based classification in QuPath software was employed to segment neurons, and pixel-based classification was utilized to identify capillaries. The centroids of the identified objects were employed in subsequent statistical analyses. A quadtree algorithm was employed to determine the nearest vessel to each identified neuron, and the distance between neuron and vessel centroids was then calculated.

Our results showed decreased distance between neurons and vasculature with increasing cortical depth. Layers 4 and 5 exhibited the shortest distances: 34.38µm and 34.03µm, respectively. This effect likely represents specialized microanatomy driven by metabolic constraints at different levels of the cortical plate, containing elements of neuronal circuits with distinct roles in visual processing and different metabolic demands.

KEYWORDS
neurovascular biology, cortical microanatomy, human neuropathology

1 | INTRODUCTION

The supply of adequate oxygen, glucose, and other metabolites to the brain, like all tissues, requires rich investment by a complex network of blood vessels. The exquisite functional control of blood flow through this network in response to brain metabolic demands, termed 'neurovascular coupling' is essential for brain tissue homeostasis and underlies a large body of knowledge driven by blood-oxygen level dependent (BOLD) imaging. While the vulnerability of brain tissue to hypoxic damage has long been recognized, the contribution of lower amplitude fluctuations in oxygen availability to brain pathophysiology have recently become appreciated, motivating closer scrutiny of the relationship between brain activity and oxygen availability. In this study, we used machine learning to analyze micrographs of human cortex in order to survey capillary density and its relationship to neuronal at each level of the cortical plate.

Abbreviations: SD, spreading depolarization; CSD, cortical spreading depression; NNCD, neuron to nearest capillary distance

1.1 | The relationship between capillary density and hypoxia

The microanatomical characteristics of brain tissue affect the patterns of susceptibility to the development of hypoxia. For instance, the hippocampus demonstrates higher sensitivity to hypoxia than does the neocortex Kirino et al. (1988). This is attributed to the differences in both vascular network structure and pericyte and endothelial cell function Shaw et al. (2021). Additionally, previous studies also demonstrate

that the neocortex and hippocampus are susceptible to transient decreases in oxygen or glucose, leading to memory loss and executive function deficits following global cerebral hypoperfusion Kirschen et al. (2017). Arterial vascularization of the hippocampus is dependent on the collateral branches of the posterior cerebral artery and the anterior choroidal artery, forming the network of superficial hippocampal arteries that in turn lead to deep intrahippocampal arteriesTatu and Vuillier (2014). Inadequacy in terms of capillary density and afferent blood vessels makes the Cornu Ammonis in the hippocampus particularly vulnerable to shortcomings in blood supply Vockert et al. (2021), Uchimura (1928).

A constant supply of oxygen and glucose from blood vessels is necessary to maintain normal homeostasis. Understanding the dynamics of the local diffusion, and how the distance to blood vessels affects neuronal excitability is crucial in developing effective treatments for migraine aura, ischemic stroke, and other neurological disease.

1.2 | The relationship between hypoxia and spreading depolarization

Hypoxia and spreading depolarization ('SD') are interconnected phenomena involved in the pathogenesis of neurological disorders such as migraine aura, traumatic brain injury, and ischemic stroke. SD describes a pathologic slow-moving (2-6 mm/min) wave that propagates through the gray matter characterized by neuronal depolarization, and disruption of intracellular and extracellular ion homeostasis. SD is followed by reduced brain electrical activity, which was first referred to in the literature as 'spreading depression' Leao (1944).

SD occurs when passive cation influx across the cell membrane exceeds the capacity of ATP-dependent Na^+ and Ca^{2+} pumps to provide outward currents preventing the generation of action potentials Cozzolino et al. (2018), Dreier (2011), Kager et al. (2002), Kraig and Nicholson (1978). The depolarization can be ignited through activation of sodium and/or calcium channels or Na/K-ATPase activity reduction Cozzolino et al. (2018), Somjen (2001), which is associated with rising K^+, or overflow of glutamate in extracellular space or conditions associated with ATP depletion Cozzolino et al. (2018). The persistent net inward current results in a reduction of electrical activity and decrease of extracellular volume due to water influx leading to intracellular hyperosmolality Cozzolino et al. (2018), Dreier (2011), Takano et al. (2007).

Brain tissue is vulnerable to ischemic stress because signal processing through action potential generation consumes a lot of energy to maintain ion gradient homeostasis Dreier (2011). During SD, both glucose and O_2 are required to restore normal ion homeostasis Lindquist (2024). Blood vessels play a contributing role in SD as a source of oxygen and nutrient supply to the affected tissue. Understanding these mechanisms is essential for targeted interventions in conditions like ischemic stroke. In healthy tissues, SD can stimulate vasodilation to increase blood flow (which is the case in migraine aura). In contrast, SD goes through triphasic neurovascular response (constriction, dilation, and then prolonged slight constriction) in pathological tissue such as that affected in ischemic stroke Kramer et al. (2016). This hypoperfusion response in pathological tissue is called the 'inverse hemodynamic response' and converts a harmless short-lasting depolarization into a harmful depolarization without repolarization. While ischemia can trigger SD, the latter can aggravate tissue hypoxia, which results in a vicious cycle of inverse hemodynamic response and hypoxia Dreier (2011).

SD is further characterized by a sharp increase in extracellular potassium and a notable decrease in pH Dreier (2011), Windmüller (2005). In normal conditions, nitric oxide (NO) counteracts potassium's vasoconstrictor effect and enhances pH-induced vasodilation, resulting in a net vasodilatory effect Golding et al. (2001). However, in cases where microvascular reactivity is disrupted, basal potassium levels rise, NO declines, and Ca^{2+}-activated K+ ('BK') channels in the neurovascular unit are activated. These responses inhibit vasodilation, and intensify vasoconstriction, thus perpetuating the cycle of ischemia and sustaining SD Windmüller (2005), Eikermann-Haerter (2014), Girouard et al. (2010). SD induces a metabolic imbalance within the ischemic penumbra by reducing blood flow and elevating energy requirements through diminished glucose and glycogen levels, along with heightened lactate production Kramer et al. (2016). Moreover, it plays a role in extending ischemia to additional susceptible tissues Sukhotinsky et al. (2008).

In vivo, SD-associated metabolic demand for O_2 can exceed supply, resulting in tissue hypoxia Takano et al. (2007), Piilgaard and Lauritzen (2009). In computational models examining the effect of O_2 availability across ex-vivo brain slices, a pathologic cycle was identified whereby SD induces, and is also exacerbated by, hypoxia Kelley et al. (2022), and depending on the distance to the O_2 bath and to the inciting K+ bolus, intermediate locations in the slice suffered various degrees of pump demand and partial pump failure. Results of the modeling experiment agreed with the in vivo experiment: tissue near capillaries resists SD, while tissue farther away is relatively hypoxic and prone to SD Takano et al. (2007).

Cortical spreading depression ('CSD') is a spatially and temporally heterogeneous phenomenon that includes a propagating wave of SD. The clinical representation of this phenomenon is widely variable, ranging from symptoms such as migraine to severe cerebral ischemia Cozzolino et al. (2018). SD can be induced in animal models, but identifying a recurring direct trigger in human brain and associating it to known pathology remains elusive. Numerous factors have been identified as triggers for SD in animal models, including electrical stimulation, potassium chloride, elevated glutamate, emboli, and astrocyte activation Charles and Baca (2013).

1.3 | The contribution of microanatomy to hypoxia

Motivated by a desire for a deeper understanding of the mechanisms by which hypoxic conditions in the human brain can influence neuronal pathology, we aimed to determine the morphologic parameters of the microcirculation in situ relative to neurons in the human cortex.

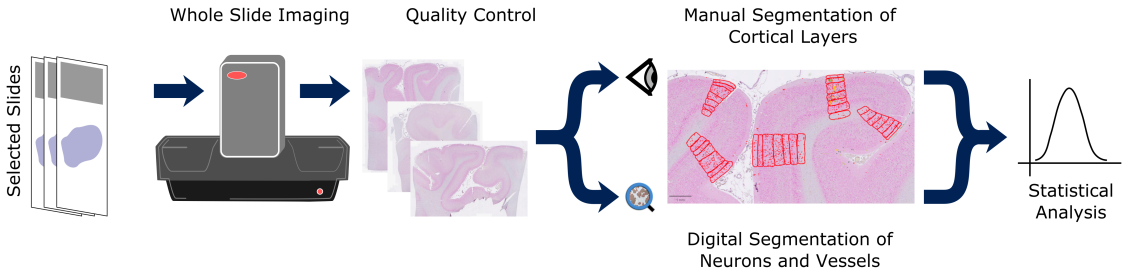

FIGURE 1 Schematic of protocol. After selection of representative slides of visual cortex from three subjects and staining with dual immunohistochemistry for CD34 (brown) and NeuN (red), digital slide images were obtained from whole slide imaging platform and manually reviewed to ensure fidelity of image acquisition. Using QuPath software, layers of the primary visual cortex in each slide were annotated manually by a neuropathologist in selected subregions with clear orientation, selected to equally cover gyral crests and sulcal depths, forming ROIs for downstream analysis. Neurons and capillaries within these ROIs were segmented using Weka trainable segmentation. Identified object measurements, including location, were exported from QuPath for statistical analysis using R.

2 | METHODS

2.1 | Histology and Whole Slide Imaging

Three cases for which neuropathologic evaluation revealed no abnormalities in the central nervous system were selected from the Yale Department of Pathology to include patients of ages 55, 65, and 75 years old. Tissue blocks containing sections of primary visual cortex in the occipital lobe were selected and new unstained slides were cut and dual-labeled with immunohistochemistry using primary antibody markers for NeuN (EMD Millipore, catalog #MAB377) to highlight neurons with secondary antibody linked to development of a red chromogen and CD34 (DAKO, catalog #M7165) to highlight vascular endothelial cells with a secondary antibody linked to development of a brown chromogen. After de-identification, all slides were scanned on a Motic EasyScan Infinity 60 imaging system (Motic Inc., Kowloon, Hong Kong) at 40X magnification, covering the whole profile of tissue on the slide at 0.26µm/pixel resolution.

2.2 | Image Segmentation and Statistical Analysis

Whole slide images were analyzed using QuPath Bankhead et al. (2017). Region of interest (ROIs) delineating cortical layers were annotated manually by a neuropathologist (MMD), across all areas of the cortex judged to be cut in a plane of section within a few degrees of perpendicular to the pial surface. Within these regions, object-based classification in QuPath Bankhead et al. (2017) was employed to segment neurons, while pixel-based classification was utilized to identify capillaries. This resulted in a total dataset of 155,231 neurons and 84,350 capillaries. The resulting segmentations underwent manual validation, and the centroids of the identified objects were employed in subsequent statistical analyses. A quadtree algorithm was employed to determine the nearest vessel to each identified neuron, and the distance between pairs of centroids was then calculated.

3 | RESULTS

3.1 | Capillary density depends on cortical depth

Across all subjects, capillary density varied across the cortical layers, with the highest average density in layer IV (484.4 per square mm) and layer III (463.6 per square mm), and lower density in layers I/II and V/VI (See Table 1 and Fig. 2B). A subject-specific effect on overall mean density was observed, with subject A showing a uniformly lower density than others, but in the same overall laminar pattern.

TABLE 1 Mean capillary density (number of capillaries per square mm) for each cortical layer and white matter across all subjects, and layer means for each subject

	All Subjects	Subj. A	Subj. B	Subj. C
Layer 1	299.4	197.3	384.4	331.0
Layer 2	398.4	270.1	430.9	453.8
Layer 3	463.6	320.6	500.7	563.4
Layer 4	484.4	430.9	542.9	507.5
Layer 5	381.9	308.4	376.7	428.2
Layer 6	327.3	302.1	377.5	299.6
White matter	123.2	110.7	176.4	112.8

3.2 | Distance of neurons to nearest capillary depends on cortical depths

The analysis of distances from neurons to the nearest capillaries (NNCD) reveals consistent patterns across subjects, despite some variability among subjects: NNCD decreases from layer I to layer IV and increase slightly in layer V and layer VI. Histograms in Fig. 3A show that layer I has the largest mean NNCD (47.9 μm), while layer IV has the shortest mean NNCD (31.7 μm). The longer error bar and the broader right-skewed distribution indicated greater variability in NNCD in layer I.

Our results also demonstrate an inverse relationship between neuronal density and neuron-vessel distance (NNCD) across cortical layers (See Fig. 3B and C). Layers II to IV, which exhibit the highest neuronal densities, also show relatively lower NNCD values, indicating closer proximity of neurons to blood vessels. Conversely, layer I, characterized by the lowest neuronal density, exhibits the largest NNCD, suggesting a greater distance between neurons and the vascular network. Despite notable variability between subjects—particularly Subject B, which shows reduced neuronal density compared to Subjects A and C—the overall trend remains consistent. These findings suggest a potential adaptation of the vascular network to neuronal metabolic demands, with closer neuron-vessel associations in regions of higher neuronal density.

3.3 | The vascular network is evenly distributed among neurons

To assess capillary-neuron proximity across cortical layers while accounting for variations in neuronal density and reducing the effect of tissue processing artifact and subject variation, we normalized the mean distance from neurons to the nearest capillaries by the mean neuronal density in each layer. The resulting normalized distances were largely consistent, in a range of 0.1 - 0.8, across cortical layers (See Fig. 4), indicating an even spatial distribution of the vascular network relative to neuronal density. Notably, layer I exhibited slightly higher normalized distances, which may reflect its lower neuronal density and greater absolute distance to capillaries. In contrast, the white matter displayed a significant increase in normalized distance and greater variability, suggesting a reduced vascular presence as well as a lower count of neurons. These findings highlight the adaptations of the vascular network that support metabolic demands across distinct cortical regions.

4 | DISCUSSION

The gross and micro-anatomy of the vascular supply of the human cortex has been the subject of much prior study, and there is substantial variation in form and location of arteries, veins, and capillaries across brain regions and between gyral crests and sulcal depths. Accurate mapping of this microanatomy is critical to the formulation and interpretation of models of numerous physiologic phenomena in humans. Our finding that layers 4 and 5 have the shortest neuron–capillary distances aligns with the high synaptic activity and integrative roles of these layers in primary visual cortex Zilles and Palomero-Gallagher (2017). This supports the idea that microvascular patterning is adapted to neuronal metabolic demand and vice-versa Ventura-Antunes and Herculano-Houzel (2022). The fact that vascular proximity is not uniform across layers, suggests that BOLD and hemodynamic signals may carry layer-specific biases. This is increasingly important for laminar fMRI studies that try to map feedforward vs. feedback signaling in human cortex Koopmans et al. (2010), Lawrence et al. (2019?).

In the pathological setting, regions with shorter or longer neuron–capillary distances may show differential vulnerability to direct ischemic damage or spreading depolarization. This provides a potential anatomical explanation for layer-selective injury patterns observed in stroke, hypoxic encephalopathy, or traumatic brain injury Rahaman and Del Bigio (2018), Takahashi et al. (1993), Sethi et al. (2006). Alterations in vascular density and vascular fragmentation have been implicated in Alzheimer's disease, vascular dementia, and small vessel disease Buée et al. (1997), Hase et al. (2019). The results and methodology presented in this work thus have implications for the physiology of hypoxia in a wide variety of neurologic diseases.

4.1 | Propagation of Spreading Depolarization

The understanding of the propagation mechanisms of SD remains incomplete. Several hypotheses rely on the diffusion of extracellular potassium or glutamate, or alternatively on the opening of neuronal or glial gap junctions Zandt et al. (2013). Current evidence suggests a growing consensus around the potassium and glutamate diffusion hypothesis, which holds that high extracellular potassium levels may be the explanation for the wave pattern of propagation Zandt et al. (2015), Pietrobon and Moskowitz (2014). Extracellular glutamate clearance can be regulated through astrocyte glutamate transporter proteins GLT-1 and GLAST, and there is evidence that glutamate transporter blockers can reduce cell excitability, SD amplitude, delay the initiation of SD, shift its spatial formation to deeper cortical layers, and reduce its propagation velocity Hosseini-Zare et al. (2017).

Like action potentials, SD waves propagate in an all-or-none fashion once triggered Cozzolino et al. (2018). SD propagates in areas surrounding an infarct where tissue remains viable, as necrotic areas are unable to support neuronal activity. The same depolarization wave varies depending on the distance from the infarct core, potentially resulting in monophasic hypoperfusion, biphasic hypoperfusion and hyperperfusion, or monophasic hyperemia Woitzik et al. (2013). SD accompanied by hypoperfusion tends to be locally restricted, which may explain why ischemic stroke typically does not manifest with migraine aura, as intrinsic mechanisms often prevent the spread of peri-infarct CSDs into distant, functional tissue. Previous studies also show that SD is more

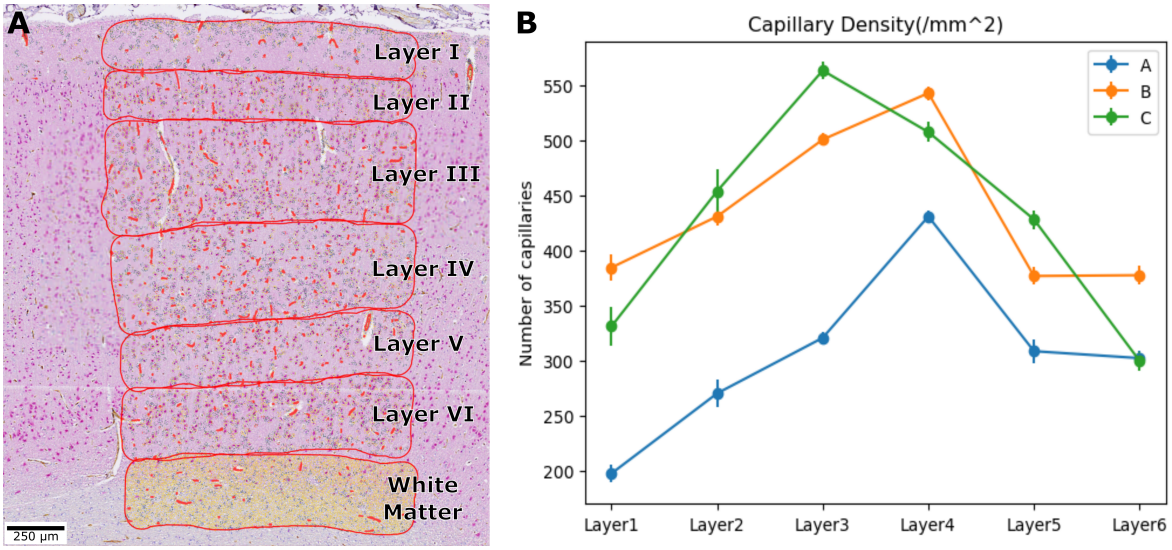

FIGURE 2 Capillary density across layers of the human primary visual cortex. (A) Representative image of the human primary visual cortex with layers I to VI and white matter outlined. Capillaries and neurons were identified and circled using QuPath software. (B) Mean capillary density plotted across cortical layers (I to VI) and white matter. Capillary density was calculated by dividing the total number of identified capillaries by the area of each region of interest (ROI). Error bars indicate variability between subjects.

difficult to elicit in the depths of sulci Bowyer et al. (1999), and propagation tends to end at a prominent sulcus, at ischemic tissue, in areas over which a previous hypoemic CSD propagated, or at major pial vessels.

4.2 | Spreading Depolarization in Neurologic Diseases

Migraine

SD has been hypothesized to be the underlying mechanism of the migraine aura. It was first noticed in humans through cerebral blood flow studies of migraine, exhibiting oligemia on the scale and timing of CSD Kramer et al. (2016), Olesen et al. (1990). Imaging studies using CT, PET, or MRI show that migraine occurs with a propagated wave of oligemia and an excitation-depression wave in patterns and with a velocity of 2 to 6 mm/min, suggestive of CSD Lauritzen et al. (2011), Woods et al. (1994), Hadjikhani (2001), Cao et al. (1999), Russell and Olesen (1996). However, obtaining direct electrophysiology recordings to further confirm this association and investigate mechanisms of initiation and propagation more deeply in humans is challenging due to the spontaneous nature of migraine attacks and the invasive procedures required.

SD can be triggered by potassium and is opposed by glial cells' ability to clear potassium Vincent (2015), and because visual aura is the most frequently reported symptom in migraine, it is believed the pathophysiology of migraine is most likely to begin in the visual cortex, which has the highest density of excitatory neurons and lowest density of astrocytes Lauritzen (1994). The propagation wave then spreads anteriorly and tends to end when reaching the central sulcus Lauritzen (1994), Bowyer et al. (1999).

Acute ischemic injuries

SD has been widely observed in patients with brain injuries or ischemic stroke Dreier (2011). For example, the Cooperative Study on Brain Injury Depolarizations (COSBID) performed invasive clinical studies on patients who had acute brain injury found that CSD propagates through both healthy and injured tissue in a large percentage of the patients Lauritzen et al. (2011). However, the triggers for cortical SD remain unidentified and unobserved.

SD occurs in the penumbra of brain infarcts, which are tissue areas that have compromised vascular and metabolic function, but are not yet irreversibly damaged Astrup et al. (1981), Nakamura et al. (2010). Research has demonstrated a correlation between the enlargement of the infarct area and the quantity of SDs Nakamura et al. (2010), Mies et al. (1993) or their total duration Dijkhuizen et al. (1999).

At the start of an acute ischemic attack, depolarization initiates and spreads at the periphery of the core Ayata (2013), Lauritzen et al. (2011), Nakamura et al. (2010). The impact of depolarization on perfusion results in significant vasoconstriction nearest to the core, hindering repolarization and expanding the core further. However, vasoconstriction is less severe or sustained further away from the core, potentially allowing repolarization but leaving the tissue vulnerable to future depolarization events. In the core region, SD manifests as a prolonged, pharmacoresistant, and more harmful wave, while in the metabolically compromised penumbra, it is shorter-lasting, more pharmacosensitive, and less harmful. In healthy tissue, the wave is more easily blocked by (e.g. by NMDA receptor antagonists alone) Somjen (2001).

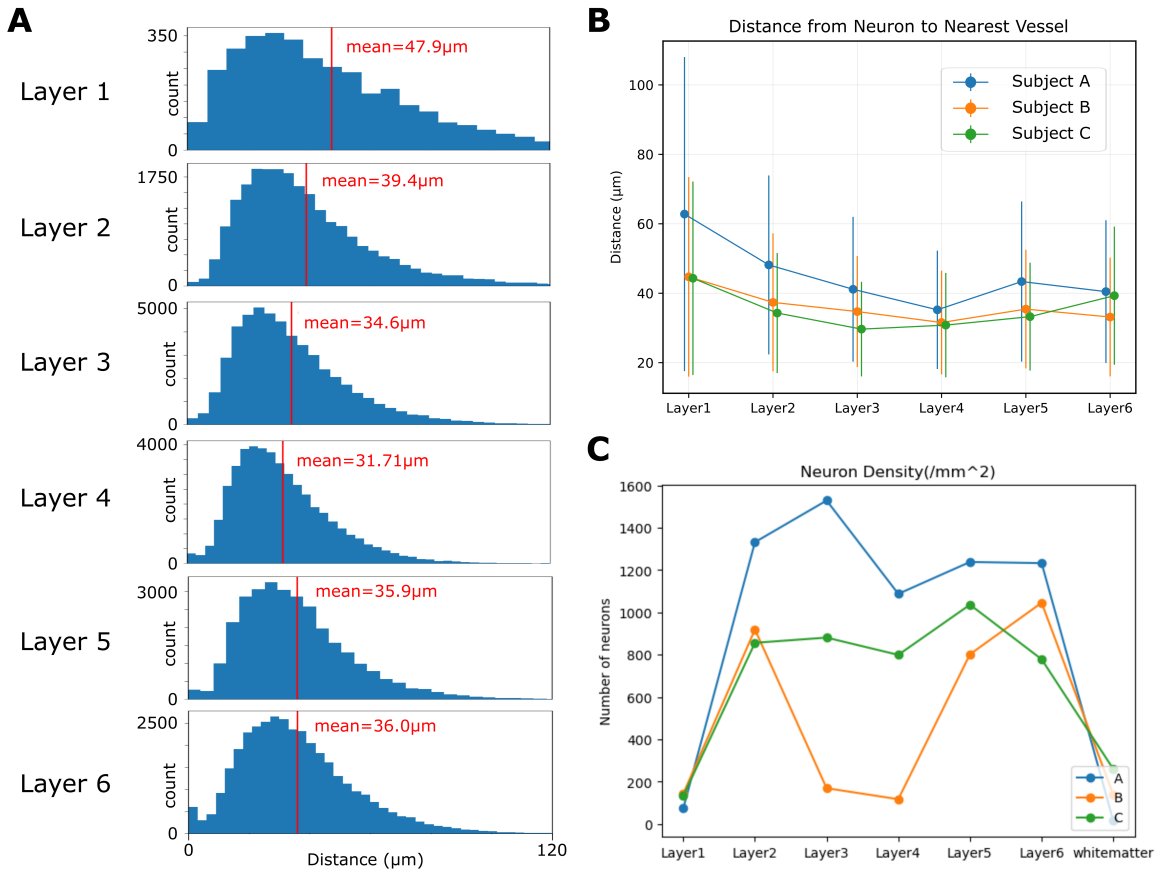

FIGURE 3 Distances from neurons to nearest capillaries across layers of the human primary visual cortex. (A) The distance from each identified neuron to its nearest neighbor capillary (NNCD) was measured, and these measurements were aggregated into separate histograms for each cortical layer. (B) Plots of mean NNCD for each cortical layer separated by subject reveal subject-level variation but similar trends across layers. Error bars=S.D. (C) The mean neuronal density for each cortical layer, plotted by subject. S.E.M.s are smaller than data point marker all points.

Chronic hypoxia

A 2024 case series study provided evidence of the occurrence of SD in a patient with moyamoya vasculopathy, suggesting that SD can be linked to the development of abnormal microvasculature in response to chronic cerebral hypoperfusion Dömer et al. (2024). Further exploration of this phenomenon is essential for comprehending how hypoxic effects can give rise to such diverse clinical manifestations. There is an increased risk of ischemic Tzourio et al. (1993), Kurth et al. (2005), Stang et al. (2005) and hemorrhagic Chang et al. (1999), Kurth et al. (2012 2010) stroke in migraine patients, especially for those with aura compared with those without. Previous research has shown that microembolic occlusion of small cerebral arteries, which can cause migraine and stroke Sevgi et al. (2012), can also induce SD in rodents Nozari et al. (2010). Moreover, migrainous stroke is a stroke that happens during migraine aura when neuroimaging shows ischemic infarction in a relevant area and the stroke is not attributed to another disorder noa (2018), suggesting that migraine can be a direct cause of ischemic stroke.

Traumatic Brain Injury

The incidence of SD among traumatic brain injury ('TBI') patients is reported to be around 50–70%, and SD often occurs in repetitive patterns over a period of at least 7 days post-trauma Hartings et al. (2011). The occurrence of SD is associated with worse clinical outcomes in patients with traumatic injury. Prolonged direct current shifts which may be triggered to arterial hypotension were observed in TBI, and may be a causative factor for secondary injury after human TBI. In research investigating the spatiotemporal dynamics and propagation of the TBI-associated CSD, it has been suggested that the injury itself may not initiate spreading depolarization waves; instead, depolarization takes place at peri-injury zones, and the injury site acts as an attractor to the depolarization waves, and sustains SD initiated by nearby, less compromised networks Hosseini-Zare et al. (2017).

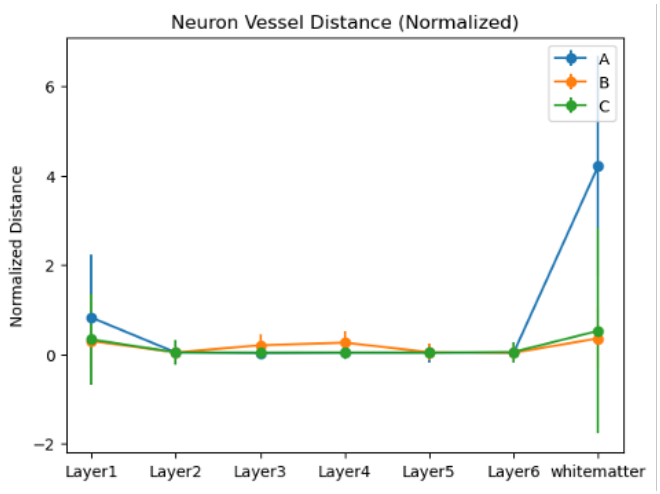

FIGURE 4 Normalized distances from neurons to nearest capillaries across layers of the human primary visual cortex. The normalized distances were calculated by dividing the mean absolute distances from neurons to their nearest capillaries by the mean neuronal density for cortical layers I to VI and white matter across subjects A, B, and C.

4.3 | Heterogeneity across regions and subjects

Capillary red-blood-cell flux and intracapillary resistance to oxygen decrease with depth, reaching a minimum around layer IV, while the depth-dependent oxygen extraction fraction is increased in layer IV. Li et al. (2019). In the mouse cortex relatively few capillaries are found immediately below the glia limitans, but capillary density increases in deeper cortical regions to an apparent maximum near 500µm below the surface of the somatosensory cortex. The rat hippocampal CA3 region was shown to be rich in microvessels, similar to the parietal or the frontal cortical regions. On the other hand, the CA1 region was shown to have a low vascular density, comparable to the corpus callosum, and capillary density is higher in the gray matter than in the white matter Wilhelm et al. (2016).

Our study focuses on analyzing the distribution of distance between neurons and vasculature in the primary visual cortex. However, additional work is essential in the study the heterogeneity of the vasculature distribution in different layers across brain regions. Intersubject variability across ages, and parameters of microcirculation accompanying specific pathologic conditions are also critical to establish in order to accurately model human disease. Our methods for pixel-based classification of whole slide images in QuPath combined with quadtree algorithms for distance mapping provide a basis for such larger surveys of human cortex across ages and conditions. This pipeline is broadly applicable to large histological datasets.

AUTHOR CONTRIBUTIONS

Study Conception and Design: W.W.L., R.A.M., M.D., Data collection and analysis: Y.W., A.G, M.D. All authors contributed to preparation and editing of the manuscript.

ACKNOWLEDGMENTS

Research supported by NIH grants R01MH086638 and K08EY033013. We thank the Yale Center for Research Computing for guidance and use of the research computing infrastructure, and the Yale Digital Pathology Working Group for guidance and use of the whole slide imaging system.

FINANCIAL DISCLOSURE

None reported.

CONFLICT OF INTEREST

The authors declare no potential conflict of interests.

REFERENCES

(2018) Headache Classification Committee of the International Headache Society (IHS) The International Classification of Headache Disorders, 3rd edition. *Cephalalgia*, 38(1), 1–211. doi:10.1177/0333102417738202, publisher: SAGE Publications Ltd STM.
URL https://doi.org/10.1177/0333102417738202

Astrup, J., Siesjo, B. & Symon, L. (1981) Thresholds in cerebral ischemia - the ischemic penumbra. *Stroke*, 12, 723–5.

Ayata, C. (2013) Spreading depression and neurovascular coupling. *Stroke*, 44(6 Suppl 1), S87–89. doi:10.1161/STROKEAHA.112.680264.

Bankhead, P., Loughrey, M.B., Fernández, J.A., Dombrowski, Y., McArt, D.G., Dunne, P.D. et al. (2017) QuPath: Open source software for digital pathology image analysis. *Scientific Reports*, 7(1), 16878. doi:10.1038/s41598-017-17204-5.
URL https://doi.org/10.1038/s41598-017-17204-5

Bowyer, S., Tepley, N., Papuashvili, N., Kato, S., Barkley, G., Welch, K. et al. (1999) *Analysis of MEG signals of spreading cortical depression with propagation constrained to a rectangular cortical strip*.

Buée, L., Hof, P.R. & Delacourte, A. (1997) Brain Microvascular Changes in Alzheimer's Disease and Other Dementias. *Annals of the New York Academy of Sciences*, 826(1), 7–24. doi:10.1111/j.1749-6632.1997.tb48457.x, _eprint: https://nyaspubs.onlinelibrary.wiley.com/doi/pdf/10.1111/j.1749-6632.1997.tb48457.x.
URL https://onlinelibrary.wiley.com/doi/abs/10.1111/j.1749-6632.1997.tb48457.x

Cao, Y., Welch, K., Aurora, S. & Vikingstad, E. (1999) Functional MRI-BOLD of visually triggered headache in patients with migraine. *Arch. Neurol*, 56, 548–554.

Chang, C., Donaghy, M. & Poulter, N. (1999) Migraine and stroke in young women: case-control study. The World Health Organisation Collaborative Study of Cardiovascular Disease and Steroid Hormone Contraception. *BMJ*, 318, 13–18.

Charles, A.C. & Baca, S.M. (2013) Cortical spreading depression and migraine. *Nature Reviews. Neurology*, 9(11), 637–644. doi:10.1038/nrneurol.2013.192.

Cozzolino, O., Marchese, M., Trovato, F., Pracucci, E., Ratto, G.M., Buzzi, M.G. et al. (2018) Understanding Spreading Depression from Headache to Sudden Unexpected Death. *Frontiers in Neurology*, 9, 19. doi:10.3389/fneur.2018.00019.

Dijkhuizen, R.M., Beekwilder, J.P., van der Worp, H.B., Berkelbach van der Sprenkel, J.W., Tulleken, K.A. & Nicolay, K. (1999) Correlation between tissue depolarizations and damage in focal ischemic

rat brain. *Brain Research*, 840(1-2), 194–205. doi:10.1016/s0006-8993(99)01769-2.

Dreier, J.P. (2011) The role of spreading depression, spreading depolarization and spreading ischemia in neurological disease. *Nature Medicine*, 17(4), 439–447. doi:10.1038/nm.2333.

Dömer, P., Helgers, S.O., Meinert, F., Sánchez-Porras, R., Mathys, C., Witt, K. et al. (2024) Cortical Spreading Depolarization in Moyamoya Vasculopathy: A Case Series. *Stroke*, 55(4), 1086–1089. doi:10.1161/STROKEAHA.123.044873, publisher: American Heart Association.
URL https://www.ahajournals.org/doi/10.1161/STROKEAHA.123.044873

Eikermann-Haerter, K. (2014) Spreading depolarization may link migraine and stroke. *Headache: The Journal of Head and Face Pain*, 54(7), 1146–1157.

Girouard, H., Bonev, A., Hannah, R., Meredith, A., Aldrich, R. & Nelson, M. (2010) Astrocytic endfoot Ca2+ and Bk channels determine both arteriolar dilation and constriction. *Proc Natl Acad Sci U S A*, 107, 3811–3816.

Golding, E., Steenberg, M., Johnson, T. & Bryan, R. (2001) Nitric oxide in the potassium-induced response of the rat middle cerebral artery: a possible permissive role. *Brain Res*, 889, 98–104.

Hadjikhani, N. (2001) Mechanisms of migraine aura revealed by functional MRI in human visual cortex. *Proc. Natl Acad. Sci. USA*, 98, 4687–4692.

Hartings, J., Watanabe, T., Bullock, M., Okonkwo, D., Fabricius, M., Woitzik, J. et al. (2011) Spreading depolarizations have prolonged direct current shifts and are associated with poor outcome in brain trauma. *Brain*, 134(5), 1529–1540.

Hase, Y., Ding, R., Harrison, G., Hawthorne, E., King, A., Gettings, S. et al. (2019) White matter capillaries in vascular and neurodegenerative dementias. *Acta Neuropathologica Communications*, 7(1), 16. doi:10.1186/s40478-019-0666-x.
URL https://doi.org/10.1186/s40478-019-0666-x

Hosseini-Zare, M., Gu, F., Abdulla, A., Powell, S. & Žiburkus, J. (2017) Effects of experimental traumatic brain injury and impaired glutamate transport on cortical spreading depression. *Exp Neurol*, 295, 155–61. doi:10.1016/j.

Kager, H., Wadman, W.J. & Somjen, G.G. (2002) Conditions for the triggering of spreading depression studied with computer simulations. *Journal of Neurophysiology*, 88(5), 2700–2712. doi:10.1152/jn.00237.2002.

Kelley, C., Newton, A.J.H., Hrabetova, S., McDougal, R.A. & Lytton, W.W. (2022) Multiscale Computer Modeling of Spreading Depolarization in Brain Slices. *eNeuro*, 9(4), ENEURO.0082–22.2022. doi:10.1523/ENEURO.0082-22.2022.

Kirino, T., Tamura, A. & Sano, K. (1988) Early and Late Neuronal Damage Following Cerebral Ischemia. In: Somjen, G. (Ed.) *Mechanisms of Cerebral Hypoxia and Stroke*. Boston, MASpringer US, pp. 23–34.
URL https://doi.org/10.1007/978-1-4684-5562-5_3

Kirschen, G.W., Kéry, R. & Ge, S. (2017) The Hippocampal Neuro-Glio-Vascular Network: Metabolic Vulnerability and Potential Neurogenic Regeneration in Disease. *Brain Plasticity*, 3(2), 129–144. doi:10.3233/BPL-170055.
URL https://www.ncbi.nlm.nih.gov/pmc/articles/PMC6091038/

Koopmans, P.J., Barth, M. & Norris, D.G. (2010) Layer-specific BOLD activation in human V1. *Human Brain Mapping*, 31(9), 1297–1304. doi:10.1002/hbm.20936.

Kraig, R.P. & Nicholson, C. (1978) Extracellular ionic variations during spreading depression. *Neuroscience*, 3(11), 1045–1059. doi:10.1016/0306-4522(78)90122-7.

Kramer, D.R., Fujii, T., Ohiorhenuan, I. & Liu, C.Y. (2016) Cortical spreading depolarization: Pathophysiology, implications, and future directions. *Journal of Clinical Neuroscience: Official Journal of the Neurosurgical Society of Australasia*, 24, 22–27. doi:10.1016/j.jocn.2015.08.004.

Kurth, T., Chabriat, H. & Bousser, M.G. (2012) Migraine and stroke: a complex association with clinical implications. *The Lancet. Neurology*, 11(1), 92–100. doi:10.1016/S1474-4422(11)70266-6.

Kurth, T., Kase, C., Schurks, M., Tzourio, C. & Buring, J. (2010) Migraine and risk of haemorrhagic stroke in women: prospective cohort study. *BMJ*, 341, 3659.

Kurth, T., Slomke, M. & Kase, C. (2005) Migraine, headache, and the risk of stroke in women: a prospective study. *Neurology*, 64, 1020–26.

Lauritzen, M. (1994) Pathophysiology of the migraine aura. The spreading depression theory. *Brain: A Journal of Neurology*, 117 (Pt 1), 199–210. doi:10.1093/brain/117.1.199.

Lauritzen, M., Dreier, J.P., Fabricius, M., Hartings, J.A., Graf, R. & Strong, A.J. (2011) Clinical relevance of cortical spreading depression in neurological disorders: migraine, malignant stroke, subarachnoid and intracranial hemorrhage, and traumatic brain injury. *Journal of Cerebral Blood Flow and Metabolism: Official Journal of the International Society of Cerebral Blood Flow and Metabolism*, 31(1), 17–35. doi:10.1038/jcbfm.2010.191.

Lawrence, S.J., Norris, D.G. & de Lange, F.P. (2019) Dissociable laminar profiles of concurrent bottom-up and top-down modulation in the human visual cortex. *eLife*, 8, e44422. doi:10.7554/eLife.44422, publisher: eLife Sciences Publications, Ltd.
URL https://doi.org/10.7554/eLife.44422

Leao, A.A.P. (1944) Spreading depression of activity in the cerebral cortex. *Journal of Neurophysiology*, 7(6), 359–390. doi:10.1152/jn.1944.7.6.359, publisher: American Physiological Society.
URL https://journals.physiology.org/doi/abs/10.1152/jn.1944.7.6.359

Li, B., Esipova, T.V., Sencan, I., Kılıç, K., Fu, B., Desjardins, M. et al. (2019) More homogeneous capillary flow and oxygenation in deeper cortical layers correlate with increased oxygen extraction. *eLife*, 8, e42299. doi:10.7554/eLife.42299.

Lindquist, B.E. (2024) Spreading depolarizations pose critical energy challenges in acute brain injury. *Journal of Neurochemistry*, 168(5), 868–887. doi:10.1111/jnc.15966.

Mies, G., Iijima, T. & Hossmann, K.A. (1993) Correlation between peri-infarct DC shifts and ischaemic neuronal damage in rat. *Neuroreport*, 4(6), 709–711. doi:10.1097/00001756-199306000-00027.

Nakamura, H., Strong, A., Dohmen, C., Sakowitz, O., Vollmar, S., Sue, M. et al. (2010) Spreading depolarizations cycle around and enlarge focal ischaemic brain lesions. *Brain*, 133, 1994–2006.

Nozari, A., Dilekoz, E., Sukhotinsky, I. & etal (2010) Microemboli may link spreading depression, migraine aura, and patent foramen ovale. *Ann Neurol*, 67, 221–229.

Olesen, J., Friberg, L., Olsen, T.S., Iversen, H.K., Lassen, N.A., Andersen, A.R. et al. (1990) Timing and topography of cerebral blood flow, aura, and headache during migraine attacks. *Annals of Neurology*, 28(6), 791–798. doi:10.1002/ana.410280610.

Pietrobon, D. & Moskowitz, M. (2014) Chaos and commotion in the wake of cortical spreading depression and spreading depolarizations. *Nat. Rev. Neurosci*, 15, 379–393.

Piilgaard, H. & Lauritzen, M. (2009) Persistent increase in oxygen consumption and impaired neurovascular coupling after spreading depression in rat neocortex. *Journal of Cerebral Blood Flow and Metabolism: Official Journal of the International Society of Cerebral Blood Flow and Metabolism*, 29(9), 1517–1527. doi:10.1038/jcbfm.2009.73.

Rahaman, P. & Del Bigio, M.R. (2018) Histology of Brain Trauma and Hypoxia-Ischemia. *Academic Forensic Pathology*, 8(3), 539–554. doi:10.1177/1925362118797728.
URL https://pmc.ncbi.nlm.nih.gov/articles/PMC6490582/

Russell, M. & Olesen, J. (1996) A nosographic analysis of the migraine aura in a general population. *Brain*, 119, 355–61.

Sethi, N.K., Torgovnick, J., Macaluso, C. & Arsura, E. (2006) Cortical laminar necrosis following anoxic encephalopathy. *Neurology India*, 54(3), 327. doi:10.4103/0028-3886.27178.
URL https://journals.lww.com/neur/fulltext/2006/54030/cortical_laminar_necrosis_following_anoxic.40.aspx?utm_source=chatgpt.com

Sevgi, E., Erdener, S., Demirci, M., Topcuoglu, M. & Dalkara, T. (2012) Paradoxical air microembolism induces cerebral bioelectrical abnormalities and occasionally headache in patent foramen ovale patients with migraine. *J. Am. Heart Assoc*, 1:e001735.

Shaw, K., Bell, L., Boyd, K., Grijseels, D.M., Clarke, D., Bonnar, O. et al. (2021) Neurovascular coupling and oxygenation are decreased in hippocampus compared to neocortex because of microvascular differences. *Nature Communications*, 12(1), 3190. doi:10.1038/s41467-021-23508-y, publisher: Nature Publishing Group.
URL https://www.nature.com/articles/s41467-021-23508-y

Somjen, G.G. (2001) Mechanisms of spreading depression and hypoxic spreading depression-like depolarization. *Physiological Reviews*, 81(3), 1065–1096. doi:10.1152/physrev.2001.81.3.1065.

Stang, P., Carson, A. & Rose, K. (2005) Headache, cerebrovascular symptoms, and stroke: the Atherosclerosis Risk in Communities Study. *Neurology*, 64, 1573–77.

Sukhotinsky, I., Dilekoz, E., Moskowitz, M.A. & Ayata, C. (2008) Hypoxia and hypotension transform the blood flow response to cortical spreading depression from hyperemia into hypoperfusion in the rat. *Journal of Cerebral Blood Flow and Metabolism: Official Journal of the International Society of Cerebral Blood Flow and Metabolism*, 28(7), 1369–1376. doi:10.1038/jcbfm.2008.35.

Takahashi, S., Higano, S., Ishii, K., Matsumoto, K., Sakamoto, K., Iwasaki, Y. et al. (1993) Hypoxic brain damage: cortical laminar necrosis and delayed changes in white matter at sequential MR imaging. *Radiology*, 189(2), 449–456. doi:10.1148/radiology.189.2.8210374, publisher: Radiological Society of North America.
URL https://pubs.rsna.org/doi/abs/10.1148/radiology.189.2.8210374

Takano, T., Tian, G.F., Peng, W., Lou, N., Lovatt, D., Hansen, A.J. et al. (2007) Cortical spreading depression causes and coincides with tissue hypoxia. *Nature Neuroscience*, 10(6), 754–762. doi:10.1038/nn1902.

Tatu, L. & Vuillier, F. (2014) Structure and Vascularization of the Human Hippocampus. In: Szabo, K. & Hennerici, M. (Eds.) *Frontiers of Neurology and Neuroscience*. Vol. 34S. Karger AG, pp. 18–25.
URL https://karger.com/books/book/245/chapter/5169395

Tzourio, C., Iglesias, S. & Hubert, J. (1993) Migraine and risk of ischaemic stroke: a case-control study. *BMJ*, 307, 289–92.

Uchimura, J. (1928) Über die Grefäßyersorgung des Ammonshornes. *Zeitschrift für die gesamte Neurologie und Psychiatrie*, 112(1), 1–19. doi:10.1007/BF02863881.
URL https://doi.org/10.1007/BF02863881

Ventura-Antunes, a. & Herculano-Houzel, S. (2022) Energy supply per neuron is constrained by capillary density in the mouse brain. *Frontiers in Integrative Neuroscience*, 16. doi:10.3389/fnint.2022.760887, publisher: Frontiers.
URL https://www.frontiersin.org/journals/integrative-neuroscience/articles/10.3389/fnint.2022.760887/full

Vincent, M.B. (2015) Vision and migraine. *Headache: The Journal of Head and Face Pain*, 55(4), 595–599.

Vockert, N., Perosa, V., Ziegler, G., Schreiber, F., Priester, A., Spallazzi, M. et al. (2021) Hippocampal vascularization patterns exert local and distant effects on brain structure but not vascular pathology in old age. *Brain Communications*, 3(3), fcab127. doi:10.1093/braincomms/fcab127.
URL https://doi.org/10.1093/braincomms/fcab127

Wilhelm, I., Nyúl-Tóth, ?., Suciu, M., Hermenean, A. & Krizbai, I.A. (2016) Heterogeneity of the blood-brain barrier. *Tissue Barriers*, 4(1), e1143544. doi:10.1080/21688370.2016.1143544, publisher: Taylor & Francis _eprint: https://doi.org/10.1080/21688370.2016.1143544.
URL https://doi.org/10.1080/21688370.2016.1143544

Windmüller, O. (2005) Ion changes in spreading ischaemia induce rat middle cerebral artery constriction in the absence of NO. *Brain*, 128, 2042–2051.

Woitzik, J., Hecht, N., Pinczolits, A., Sandow, N., Major, S., Winkler, M.K.L. et al. (2013) Propagation of cortical spreading depolarization in the human cortex after malignant stroke. *Neurology*, 80(12), 1095–1102. doi:10.1212/WNL.0b013e3182886932.

Woods, R., Iacoboni, M. & Mazziotta, J. (1994) Bilateral spreading cerebral hypoperfusion during spontaneous migraine headache. *N. Engl. J. Med*, 331, 1689–1692.

Zandt, B.J., Haken, B., Putten, M. & Dahlem, M. (2015) How does spreading depression spread? Physiology and modeling. *Rev Neurosci*, 26, 183–98. doi:10.1515/revneuro-2014-0069.

Zandt, B.J., Stigen, T., Ten Haken, B., Netoff, T. & Putten, M. (2013) Single neuron dynamics during experimentally induced anoxic depolarization. *J Neurophysiol*, 110, 1469–75. doi:10.1152/jn.00250.2013.

Zilles, K. & Palomero-Gallagher, N. (2017) Multiple Transmitter Receptors in Regions and Layers of the Human Cerebral Cortex. *Frontiers in Neuroanatomy*, 11. doi:10.3389/fnana.2017.00078, publisher: Frontiers.
URL https://www.frontiersin.org/journals/neuroanatomy/articles/10.3389/fnana.2017.00078/full